Radiative deflection of a BaF molecular beam via optical cycling

Tao Chen, Wenhao Bu, and Bo Yan*

Department of Physics, Zhejiang University, Hangzhou 310027, China and Collaborative Innovation Center of Advanced Microstructures, Nanjing 210093, China

(Received 24 September 2017; published 6 November 2017)

We demonstrate a quasioptical cycling for the $X(v=0) \rightarrow A(v'=0)$ transition and a radiative force-induced deflection on the buffer-gas-cooled BaF molecular beam. The laser-induced fluorescence enhancement with additional sidebands and a polarization modulation scheme indicates that the hyperfine states and the Zeeman sublevels are closed. The quasioptical cycling by repumping the $X(v=1) \rightarrow A(v'=0)$ leads to an ~0.8-mm deflection of the beam via scattering ~150 photons per molecule, in good agreement with the predictions from our multilevel rate equation model. Further improvement by closing the leakage $X(v=2)$ and Δ state allows scattering of thousands of photons and laser cooling and slowing of BaF.

DOI: 10.1103/PhysRevA.96.053401

I. INTRODUCTION

Laser cooling and trapping [1] using the light scattering force have led to many fundamental breakthroughs in atomic and quantum physics, especially the frequency standard for precision measurement [2] and the applications of the degenerate quantum gases [3,4]. Over the past decade, great effort has been put into extending the techniques for control and cooling neutral atoms to polar molecules [5,6] due to the additional vibrational rotational degrees of freedom, which provide potential novel applications in many-body physics [7,8], cold controlled chemistry [9,10], and quantum simulation and computation [11–13]. While high phase-space density has been achieved in closed-shell bi-alkali-metal molecules by external association and adiabatic transferring techniques [14,15], producing a degenerate open-shell molecular sample, such as an alkali-metal–alkaline-earth-metal system, is still under exploration [16,17]. In addition, another type of open-shell molecule, alkaline-earth-metal monohydride and monofluoride, first proposed by Di Rosa [18], can be directly laser cooled [19], which has received quite a bit of interest in recent years.

In fact, for molecules, it is difficult to find a perfect closed optical cycling channel to provide successive photon-molecule interactions required by laser cooling because of the additional complexities. Fortunately, molecules like alkaline-earth-metal monohydride and monofluoride have special internal level structures, leading to a nearly diagonal distribution of the Franck-Condon factors (FCFs), which results in a much simpler repumping process [18], making laser cooling feasible. The earlier experimental demonstrations of laser cooling such molecules (SrF [19,20] and YO [21]) were implemented by DeMille and co-workers and Yeo *et al.*, respectively, following which the magneto-optical trapping of these two molecules was achieved a short time later [22–24]. Until now, on the one hand, the temperature of the trapped molecule samples has been achieved lower and lower, and recently a three-dimensional molasses of sub-Doppler temperature (50 μK) was produced for the CaF molecule [25]. On the other hand, increasing the density of the molecular samples is urgent for further experiments, such as evaporative cooling or sympathetical cooling. Molecular densities of 2.3×10^5 cm^{-3} [25] and 4×10^6 cm^{-3} [26] were achieved by Truppe *et al.* and Anderegg *et al.*, respectively. Besides these significant advances, laser-cooling exploration on other molecules has sprung up, including YbF [27], MgF [28], and BaH [29], and now even Sisyphus cooling of polyatomic molecule (SrOH) has been achieved [30].

Besides the above, the BaF molecule is another candidate for direct laser-cooling and -trapping experiments due to the similar level structures and the good transition wavelength (~900 nm) that can be easily achieved with external cavity diode lasers [31]. Besides, the effective buffer-gas cooling of BaF to several lowest-lying rovibrational levels required by laser cooling has already been demonstrated [32]. Recently, a rovibrational cooling of a supersonic BaF beam to a rotational temperature of ~6 K with broadband laser sources has also been reported [33], which provides another possible approach for preparing the molecular source for laser cooling and trapping, although the forward velocity is rather large and hard to slow down.

In this paper we demonstrate experimentally the quasicycling transition and further observe the light scattering force-induced deflection on the buffer-gas-cooled BaF molecular beam. We use the $X\,^2\Sigma_{1/2} \rightarrow A\,^2\Pi_{1/2}$ electronic transition (with the linewidth $\Gamma = 2\pi \times 2.84$ MHz [34]), which has the required highly diagonalized FCFs, to close the vibrational branching. The cycling scheme has been described in detail in Ref. [35]. The $N = 1 \rightarrow J' = 1/2$ rotational transition is employed to eliminate the rotational branching and a sideband modulation scheme is used to generate four frequency branches to cover the hyperfine levels. In the present experiment, we have not yet taken into account the leakage channel from the $A'\,^2\Delta$ state. The paper is organized as follows. Section II describes the experimental details. In Sec. III we present the enhancement of the laser-induced fluorescence (LIF) by introducing the $X(v=1) \rightarrow A(v'=0)$ repump laser, the sideband modulation, and the polarization modulation of the light. Furthermore, we show the deflection of the molecular beam induced by the quasicycling photon scattering. Section IV gives a brief conclusion and outlook.

*yanbohang@zju.edu.cn

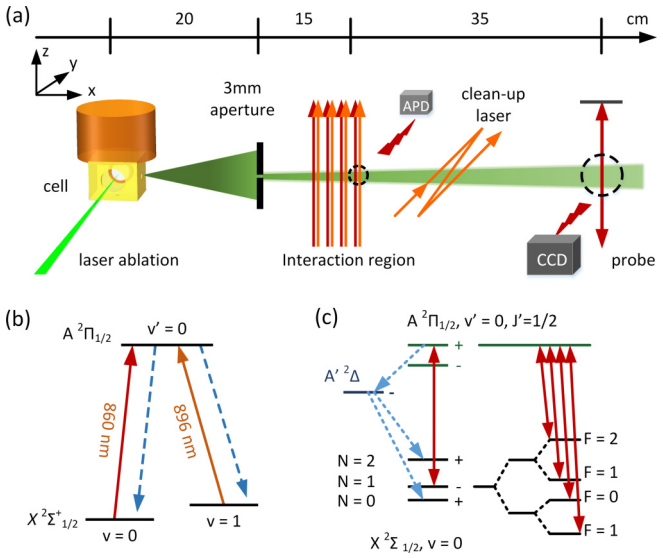

FIG. 1. Experimental setup and the molecular energy levels involved. (a) Schematic picture of the experiment. A cold BaF molecular beam along the $+\hat{x}$ direction is produced by laser ablation on a BaF_2 target followed by buffer-gas cooling with 4 K He gas in the cell; then it enters the interaction region via a 3-mm aperture. The laser beams containing both a pump (860 nm, red) and repump (896 nm, orange) pass through the interaction region along the $+\hat{z}$ direction and an avalanche photodiode (APD) is employed to collect the fluorescence from the beam. The clean-up laser along the $\hat{y}$ direction pumps the molecules from the $X(v = 1)$ state back into the $X(v = 0)$ ground state. Finally, the molecular beam profiles are imaged by a CCD camera along the $\hat{y}$ direction at 35 cm downstream from the interaction region. (b) Vibrational level structure of BaF. A repump laser of 896 nm for $X(v = 1) \rightarrow A(v' = 0)$ is used in our experiment. (c) Rotational and hyperfine structures. Both the pump and repump lasers are sideband modulated to address all four hyperfine levels of $X(N = 1)$.

II. EXPERIMENT

Figure 1(a) shows a diagram of the deflection experiment. We demonstrate the cycling scheme based on the buffer-gas-cooled molecular beam of BaF produced with the laser ablation. Different from our previous study of the cold collisions between BaF and He [32], the He buffer gas here flows into the cell at a rate of 2 standard cubic centimeters per minute. The effectively thermalized (∼4 K) mixture of He and BaF forms a beam via a 3-mm exit aperture of the cell. Another 3-mm aperture lying 20 cm downstream from the cell filters out the molecules with higher transverse velocity and collimates the beam. To deflect the molecules, we apply several laser beams along the $\hat{z}$ direction, perpendicular to the beam propagation. The molecule-light interaction time is controlled just by varying the pass number of the beams; the maximum pass number can be tuned to 8 in our experiment. The pump (860 nm) and repump (896 nm) lasers [see Fig. 1(b)] are spatially overlapped with a diameter of $d = 2$ mm and powers of 160 and 100 mW, respectively. To make all passes along the same direction, the laser beams are circularly reflected around the vacuum chamber [20] with four coated mirrors. The LIF from the $A(v' = 0) \rightarrow X(v = 0)$ transition is collected by an avalanche photodiode (APD), which focuses on the first laser beam in the 10-cm-long interaction region. The deflection probe region is located $D = 35$ cm away from the interaction region and between them a clean-up laser (896 nm) with a diameter of 8 mm and power of 50 mW hits the molecular beam to pump the molecules from the $X(v = 1)$ state back to the $X(v = 0)$ state. The BaF molecular beam profiles, including the width and position, are recorded by imaging LIF from a retroreflected laser beam (only 860 nm) on a CCD camera in probe region. The zoom ratio of the image system is 3:1. A band-pass filter of 860 ± 10 nm is used to decrease the background noise from the ablation laser and other stray lights.

To eliminate the hyperfine dark state, both the pump and repump lasers should cover all four hyperfine levels of the $X(N = 1)$ states [see Fig. 1(c)]. Recalling the analysis in Ref. [35], a resonant-type electro-optic modulator with a modulation frequency of 38 MHz is employed in our experiment and a modulation depth of 2.6 results in the first and second sidebands with equal amplitude, nearly matching the four hyperfine transitions in $X(N = 1, -) \rightarrow A(J' = 1/2, +)$. In contrast, the Zeeman dark state could be remixed by applying either an angled magnetic field or time-dependent polarization modulation [36]. Here we use a Pockels cell to implement the polarization switching scheme and the modulation frequency is set as 1 MHz. Additionally, both the clean-up and the deflection probe beams are sideband modulated and polarization modulated as well.

III. RESULTS AND DISCUSSION

A. Quasioptical cycling

Figure 2 shows the time of flight (TOF) LIF signals from the main pump transition monitored by the APD with the toggle technique applied. For LIF detection, only one single deflection laser beam passes through the interaction region. We recorded every two LIF signals in series; they are under the conditions with and without one parameter (say, the repump or the modulation, etc.), respectively. From Fig. 2(a), by introducing the 38-MHz sideband modulation to the pump laser to address the hyperfine sublevels, the LIF signal is ∼2.5× enhanced in comparison with that when only one single-frequency pump laser resonant with the $F = 2$ sublevel is applied. This can be easily understood since many more sublevels are excited by the additional sidebands, leading to more scattering photons before the molecules populate the Zeeman dark states and the $X(v = 1)$ state. On the other hand, the TOF signal tells us the time window of the detection, i.e., the interaction time between the molecular beam and the laser. The peak LIF signal appears at ∼1.7 ms, while the ablation laser fires at 0 ms and the distance between the cell and the interaction region is 35 cm, indicating that the most probable velocity is $u_0 \approx 200$ m/s. This means that the time window of the APD is about $\tau = d/u_0 = 10$ μs.

The addition of the time-dependent 1-MHz polarization modulation to the pump laser increases the LIF signal by a factor of ∼1.5 [see Fig. 2(b)]. We find that the enhancement seems insensitive to the modulation frequency; a 5-MHz modulation also leads to a similar result. However, our 4+13 multilevel rate equation (MLRE) model with the experimental

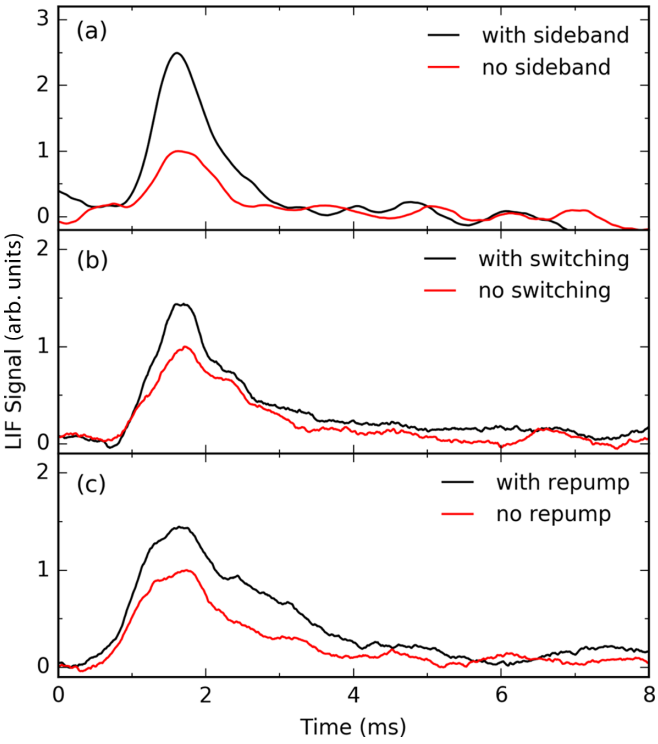

FIG. 2. Plot of LIF enhancement to demonstrate the quasioptical cycling. (a) Applying sidebands to the pump laser leads to the LIF enhancement by a factor of ∼2.5. The red (lower) line indicates the APD signal when the frequency of the pump laser hits the $F = 2$ sublevel. (b) The addition of polarization switching to both the pump and repump lasers to remix Zeeman sublevels leads to ∼1.5× enhancement. (c) The addition of $X(v = 1) \rightarrow A(v' = 0)$ to the repump laser results in another ∼1.5× enhancement of the LIF signal, indicating the cycling of the vibrational levels. All three group signals are normalized with the peak values of the red (lower) signals, respectively, and are averaged for hundreds of times to improve the signal-to-noise ratio.

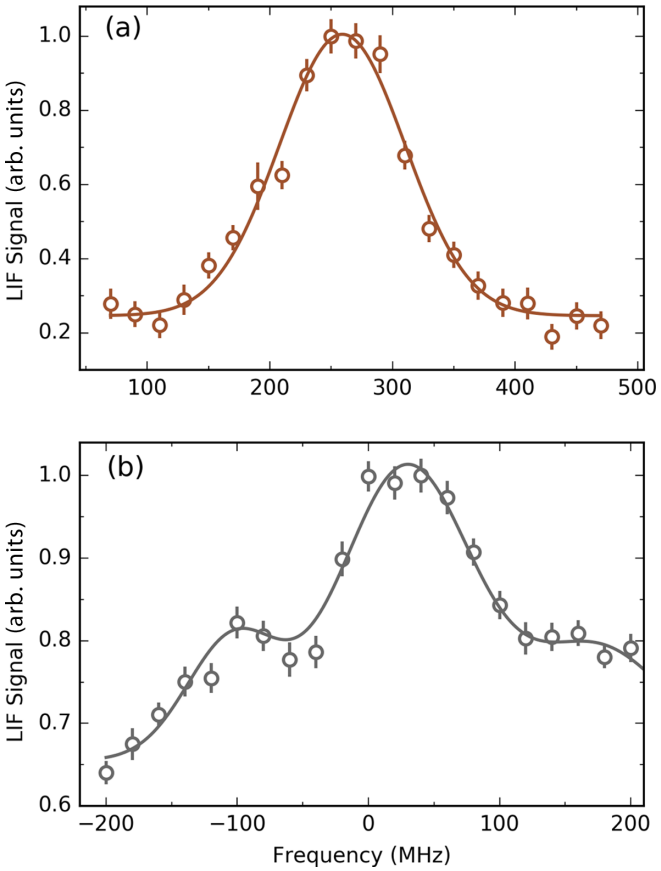

FIG. 3. Dependence of the LIF intensity on the laser frequency for (a) the 860-nm pump laser and (b) the 896-nm repump laser. The frequency scan was performed with a 38-MHz sideband modulation. For the pump laser scan, no repump laser was introduced, while for the repump scan, the pump laser was locked at the optimal point +270 MHz. The solid lines are Gaussian fits to the data points, respectively, and we lock the lasers at the frequency for the peak: 11 630.0848 cm^{-1} for the 860-nm laser and 11 164.3414 cm^{-1} for the 896-nm laser.

parameters in Sec. II indicates about 3× enhancement of the scattering photon number per molecule within the interaction time $\tau = 10\ \mu s$ (see the Appendix for details). Due to the strong pump laser intensity (the saturation factor s for each sideband is ∼300), the interaction time of 10 μs is enough to pump the molecule to the dark $X(v = 1)$ state; the model shows that each molecule scatters about 18 photons, which is close to the predicted value of $N_{00} \sim 1/(1 - q_{00}) \approx 20$, where $q_{00} = 0.9508$ [35] is the FCF for the $X(v = 0) \rightarrow A(v' = 0)$ transition. Consequently, the LIF enhancement with polarization switching indicates that about 18/1.5 = 12 photons are scattered when no switching scheme is applied. This might resort to the earth's magnetic field, which can also remix the Zeeman sublevels, since from the 4+13 model we expect that only 6 photons are scattered before the molecule populates the Zeeman dark states or $X(v = 1)$ state without any remixing technique involved.

As shown in Fig. 2(c), the addition of the $X(v = 1) \rightarrow A(v' = 0)$ repump laser further makes the LIF signal ∼1.5× enhanced. This indicates that the scattering photon number within $\tau = 10\ \mu s$ increases to 18 × 1.5 = 27, which is consistent with the predicted value from the 4+25 MLRE model with the polarization switching scheme (see Fig. 6 in Appendix). Until now, the quasioptical cycling has been implemented by applying the 38-MHz sideband modulation, the 1-MHz polarization switching scheme, and the $v = 1$ repump laser to close the hyperfine, the Zeeman, and the first vibrational dark states, respectively. The observed LIF enhancement agrees well with the predictions from our theoretical models.

Another important issue for the deflection experiment is the frequency of the pump and repump lasers. Because of the different excitation rates (related to the laser detunings) for each hyperfine sublevel in $X(N = 1)$, we scan the frequency within several hundred megahertz to find an optimal position to lock the frequency of the two lasers, respectively. Figure 3 illustrates the dependence of the LIF signal intensity (the peak value of the TOF signal) on the laser frequency with the 38-MHz sideband modulation. For the pump laser, the fit tells us that the lock point should be +270 MHz, corresponding to 11 630.0848 cm^{-1} (identical to the value resolved from the in-cell spectroscopy [32]), while for the repump laser, the best point is +30 MHz, corresponding to 11 164.3414 cm^{-1}. The

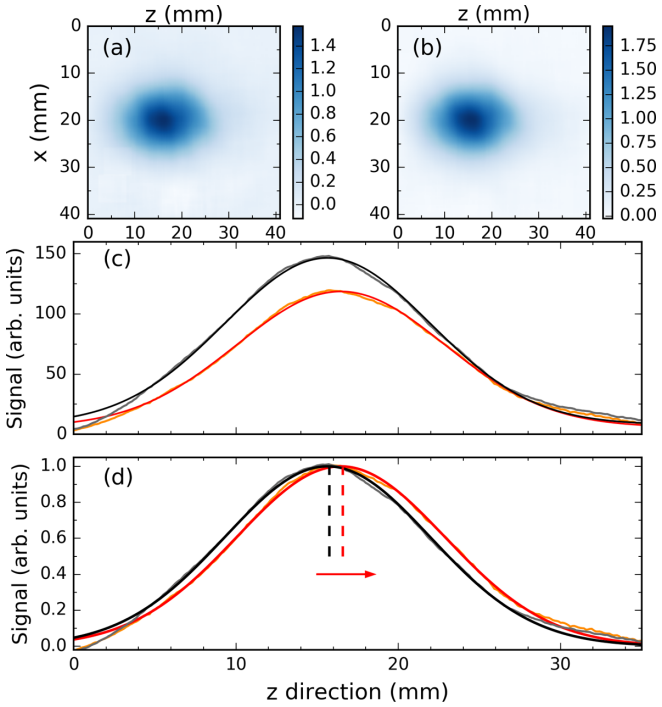

FIG. 4. Deflection of the BaF molecular beam from the quasioptical cycling. Images are given on the x-z plane of the (a) deflected and (b) unperturbed molecular beams, respectively. The $\hat{x}$ direction reflects the width of the probe laser beam, while the $\hat{z}$ direction gives the transverse profile of the molecular beam. (c) Integrated signal of the images in (a) and (b) along the $\hat{x}$ axis. The black and red lines are Gaussian fits to the unperturbed (light gray) and deflected (light orange) signal, which gives the revival rate of 80%. (d) Normalized plot of the signals in (c) to clearly show the deflection effect. The width of the molecular beam remains ~3 cm with the deflection beams applied.

clean-up laser and probe laser in Fig. 1 are also locked at these two frequency points, respectively [31].

B. Radiative deflection

The LIF enhancement for a single pass of the deflection beam in the interaction region indicates a significant radiative force on the molecules once the pass number n increases. Figure 4 shows the resolved molecular beam deflection along the $\hat{z}$ direction monitored by the CCD camera for the pass number $n = 8$. The shapes of the deflected and the unperturbed beams in the probe region are illustrated as Figs. 4(a) and 4(b), respectively. An integration of the unperturbed image along the $\hat{x}$ axis resolves the transverse width of the BaF molecular beam, about 3 cm, as shown in Fig. 4(c). The addition of the deflection beam and clean-up beam leads to a ~0.8-mm shift in the $+\hat{z}$ direction, while the beamwidth remains about 3 cm [see the normalized signals in Fig. 4(d)] . We have also tested the effect of the $X(v = 1) \rightarrow A(v' = 0)$ repump laser and clean-up laser, without which only ~10% of the molecules remain in the $X(v = 0)$ state after suffering the $X(v = 0) \rightarrow A(v' = 0)$ pump in the interaction region. Putting the repump and clean-up laser into the system again recovers the molecular signal to ~80%, which indicates effective optical pumping and

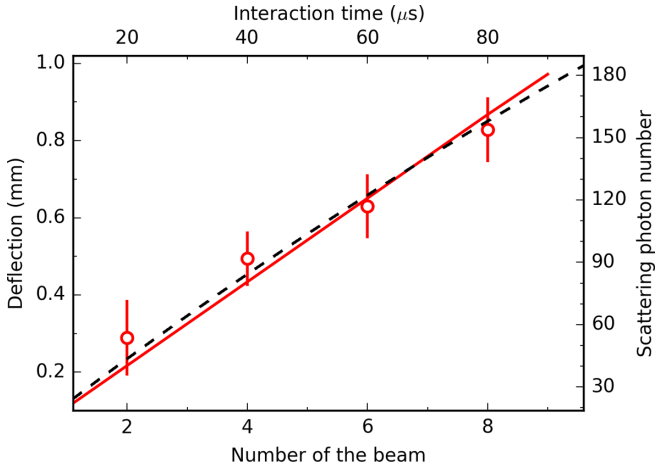

FIG. 5. Deflection distance as a function of the number of the deflection beam, yielding the dependence of the scattering photon number on the interaction time. The red solid line is a linear fit to the measured data, illustrating that the photon scattered linearly increases with the interaction time. The black dashed line is the numerical prediction of the scattering from the 4+25 MLRE model with the switching scheme, which is highly consistent with the measured data.

repumping. The 20% loss is due to the leakage $X(v \geqslant 2)$ and the $A'^2\Delta$ channels [35].

Let us make an estimation of the scattering photon number N_{sc} from the deflection length l. The time required for the molecular beam to propagate from the interaction region to the probe region is $\sim D/u_0$; then the transverse velocity changes by $\delta u = u_0 l/D$. The photon recoil momentum is given by $p = h/\lambda$, where h is Planck's constant and $\lambda = 860$ nm is the wavelength of the main pump transition. The observed deflection length $l \approx 0.8$ mm corresponds to a scattering photon number $N_{sc} = m\delta u/p \approx 150$, where m is the mass of the BaF molecule.

We have also measured the dependence of the scattered photon number N_{sc} on the interaction time $t = n\tau$, simply derived from the deflection length l versus the pass number n of the deflection beam, as shown in Fig. 5. A decrease of the pass number results in a linear decrease of the scattering photon number. The fit tells us the average scattering rate $\Gamma_{sc} =$ 2 MHz, which is only a little different from the numerical result (also plotted in Fig. 5) predicted by the 4+25 MLRE model with the switching scheme. In contrast, the theoretical maximum scattering rate for a multilevel 4+24 system [25] is given as $\Gamma_{max} = \Gamma/7 \approx 2.5$ MHz. The unsaturated average scattering rate in our experiment might result from the detunings [35] of the sidebands for the hyperfine transitions.

IV. CONCLUSION

We have shown clear evidence of the quasioptical cycling and further the radiative force from the ~150 scattering photons with only one additional $X(v = 1) \rightarrow A(v' = 0)$ repump. By applying the 38-MHz sideband modulation to the pump and repump lasers, the hyperfine dark states are eliminated. For Zeeman dark states, we have employed the 1-MHz polarization switching scheme to remix them to the cycling. Putting all these techniques together and increasing

the pass number of the beam to achieve a longer interaction time, we have observed a significant transverse deflection (∼0.8 mm) of the BaF molecular beam, indicating a scattering rate of ∼2 MHz, which agrees well with the theoretical prediction from our MLRE model.

By adjusting the detunings of the pump and repump lasers, retroreflecting both laser beams, and providing a sufficient interaction length, the molecular beam should be transversely cooled. Furthermore, the scattering photon number required for loading the beam to a trap is about $mu_0/p \approx 6.5 \times 10^4$ with a frequency chirped or white light to longitudinally slow the beam. Meanwhile, another transition, for example, $X(v=0) \rightarrow B(v''=0)$ or $C(v''=0)$, might be employed to improve the scattering force [37] in future laser slowing experiment. To build a magneto-optical trapping (MOT) of BaF, the addition of the $X(v=2) \rightarrow A(v'=1)$ repump laser should be required due to the calculated branching ratio of $\sim 1.5 \times 10^{-3}$ for $A(v'=0) \rightarrow X(v=2)$ [35] that is larger than those of CaF [38] and SrF [20]. Besides the rf MOT with polarization switching [26], our previously proposed microwave mediated MOT [39] might be another candidate for future laser-cooling and -trapping experiments.

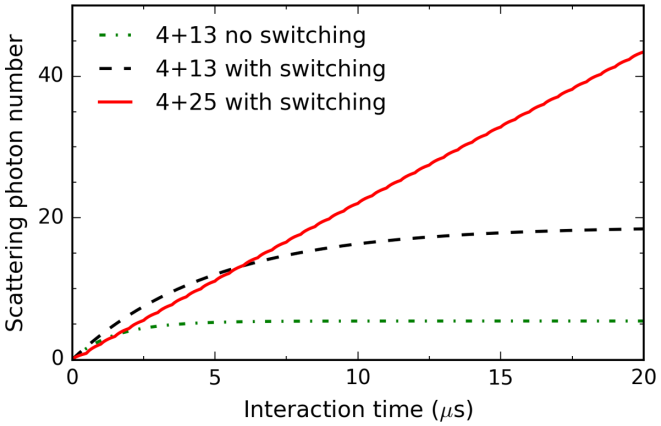

FIG. 6. Predicted scattering photon number as a function of the interaction time within 20 μs. The values are rapidly saturated for the 4+13 model, even with the polarization switching scheme to eliminate the Zeeman dark state. With both the switching scheme and $X(v=1)$ repump, the 4+25 model shows a linear relation between scattering photon number and interaction time, but the number saturates to ∼600 with a rather longer interaction time (not plotted in the figure).

ACKNOWLEDGMENTS

We acknowledge support from the National Natural Science Foundation of China under Grant No. 91636104, Zhejiang Provincial Natural Science Foundation under Grant No. LZ18A040001, and the Fundamental Research Funds for the Central Universities Grant No. 2016QNA3007. We thank Y. Xia for useful discussions.

APPENDIX: MULTILEVEL RATE EQUATION MODEL

The rate equations to describe the time evolution of the populated fraction in each sublevel for a multilevel system is given as [40]

$$\frac{dN_l}{dt} = \Gamma \sum_u r_{l,u} N_u + \sum_{u,p} R_{l,u,p}(N_u - N_l),$$
$$\frac{dN_u}{dt} = -\Gamma N_u + \sum_{l,p} R_{l,u,p}(N_l - N_u), \qquad \text{(A1)}$$

where N_l and N_u are the populated fractions for the lth sublevel in the ground state and the uth sublevel in the excited state, Γ is the spontaneous decay rate of the excited state, $r_{l,u}$ is the branching ratio for $u \rightarrow l$ transitions (see the values in Ref. [35]), and $R_{l,u,p} = \frac{\Gamma}{2} \frac{r_{l,u} s_p}{1+(2\Delta_p/\Gamma)^2}$ is the excitation rate for the $l \rightarrow u$ transition from the pth laser beam [41], with s_p the saturation factor and Δ_p the detuning. For the evaluation of $R_{l,u,p}$ with the polarization switching scheme, we should take the selection rules into account, i.e., $R_{l,u,p} = 0$ for $m_u = m_l + 1$ when $\sigma_p = \sigma_-$ and $m_u = m_l - 1$ when $\sigma_p = \sigma_+$. The scattered photon number at time t_0 is evaluated from $N_{sc}(t_0) = \sum_u \int_0^{t_0} q_{00} \Gamma N_u dt$.

We first build a 4+13 model with linearly polarized laser applied, considering four excited states in $A(v'=0, J'=1/2,+)$ and 12 sublevels in $X(v=0, N=1)$. The 13th level is the assumed loss channel with a branching ratio of $q_{loss} = 1 - q_{00} = 0.05$. For linearly polarized excitation, the $X(v=0, N=1, F=2, m_F=\pm 2)$ sublevels are dark states. Our numerical calculation indicates that the molecule will be lost to the 13th level or populate the Zeeman dark states just after scattering approximately six photons (see Fig. 6). By introducing the 1-MHz polarization modulation, the model shows that the scattered photon number increases to ∼20, three times larger than that without switching, before the molecule entirely populates the dark states.

To close the loss channel, we add the $X(v=1) \rightarrow A(v'=0)$ repump laser to our model, i.e., the 4+25 model. Besides the four excited states and 12 sublevels for $X(v=0, N=1)$ and $X(v=1, N=1)$, respectively, the other loss channels, for example, $X(v \geqslant 2)$ and $A'^2\Delta$ states, are all labeled as the 25th level with a total branching ratio $q_{loss} = 1 - q_{00} - q_{01} = 1.6 \times 10^{-3}$. This model indicates that the molecule maintains nearly successive photon scattering within 100 μs (larger than the interaction time in our deflection experiment) and finally the scattering process terminates after ∼600 photons (close to the value of $1/q_{loss}$) are scattered for an interaction time of about 1 ms. Figure 6 shows the scattering photon number as a function of the interaction time within 20 μs. For a 10-μs interaction time, the addition of the $X(v=1)$ repump laser only increases the scattering number by a factor of ∼1.5, which is consistent with our experimental observation. Finally, to achieve laser cooling of BaF, the addition of the $X(v=2)$ repump laser and microwave remixing of $\Delta \rightarrow X(N=0,2)$ channels [35] is necessary to scatter thousands of photons.

[1] S. Chu, Rev. Mod. Phys. **70**, 685 (1998).

[2] A. D. Ludlow, M. M. Boyd, J. Ye, E. Peik, and P. O. Schmidt, Rev. Mod. Phys. **87**, 637 (2015).

[3] I. Bloch, J. Dalibard, and W. Zwerger, Rev. Mod. Phys. **80**, 885 (2008).
[4] S. Giorgini, L. P. Pitaevskii, and S. Stringari, Rev. Mod. Phys. **80**, 1215 (2008).
[5] L. D. Carr, D. DeMille, R. V. Krems, and J. Ye, New J. Phys. **11**, 055049 (2009).
[6] S. A. Moses, J. P. Covey, M. T. Miecnikowski, D. S. Jin, and J. Ye, Nat. Phys. **13**, 13 (2017).
[7] D.-W. Wang, M. D. Lukin, and E. Demler, Phys. Rev. Lett. **97**, 180413 (2006).
[8] H. P. Buchler, A. Micheli, and P. Zoller, Nat. Phys. **3**, 726 (2007).
[9] R. V. Krems, Phys. Chem. Chem. Phys. **10**, 4079 (2008).
[10] S. Ospelkaus, K.-K. Ni, D. Wang, M. H. G. de Miranda, B. Neyenhuis, G. Quéméner, P. S. Julienne, J. L. Bohn, D. S. Jin, and J. Ye, Science **327**, 853 (2010).
[11] D. DeMille, Phys. Rev. Lett. **88**, 067901 (2002).
[12] P. Rabl, D. DeMille, J. M. Doyle, M. D. Lukin, R. J. Schoelkopf, and P. Zoller, Phys. Rev. Lett. **97**, 033003 (2006).
[13] A. Andre, D. DeMille, J. M. Doyle, M. D. Lukin, S. E. Maxwell, P. Rabl, R. J. Schoelkopf, and P. Zoller, Nat. Phys. **2**, 636 (2006).
[14] K.-K. Ni, S. Ospelkaus, M. H. G. de Miranda, A. Pe'er, B. Neyenhuis, J. J. Zirbel, S. Kotochigova, P. S. Julienne, D. S. Jin, and J. Ye, Science **322**, 231 (2008).
[15] S. A. Moses, J. P. Covey, M. T. Miecnikowski, B. Yan, B. Gadway, J. Ye, and D. S. Jin, Science **350**, 659 (2015).
[16] H. Hara, Y. Takasu, Y. Yamaoka, J. M. Doyle, and Y. Takahashi, Phys. Rev. Lett. **106**, 205304 (2011).
[17] B. Pasquiou, A. Bayerle, S. M. Tzanova, S. Stellmer, J. Szczepkowski, M. Parigger, R. Grimm, and F. Schreck, Phys. Rev. A **88**, 023601 (2013).
[18] M. D. Di Rosa, Eur. Phys. J. D **31**, 395 (2004).
[19] E. S. Shuman, J. F. Barry, and D. DeMille, Nature (London) **467**, 820 (2010).
[20] E. S. Shuman, J. F. Barry, D. R. Glenn, and D. DeMille, Phys. Rev. Lett. **103**, 223001 (2009).
[21] M. T. Hummon, M. Yeo, B. K. Stuhl, A. L. Collopy, Y. Xia, and J. Ye, Phys. Rev. Lett. **110**, 143001 (2013).
[22] J. F. Barry, D. J. McCarron, E. B. Norrgard, M. H. Steinecker, and D. DeMille, Nature (London) **512**, 286 (2014).
[23] M. Yeo, M. T. Hummon, A. L. Collopy, B. Yan, B. Hemmerling, E. Chae, J. M. Doyle, and J. Ye, Phys. Rev. Lett. **114**, 223003 (2015).
[24] E. B. Norrgard, D. J. McCarron, M. H. Steinecker, M. R. Tarbutt, and D. DeMille, Phys. Rev. Lett. **116**, 063004 (2016).
[25] S. Truppe, H. J. Williams, M. Hambach, L. Caldwell, N. J. Fitch, E. A. Hinds, B. E. Sauer, and M. R. Tarbutt, Nat. Phys. (unpublished).
[26] L. Anderegg, B. L. Augenbraun, E. Chae, B. Hemmerling, N. R. Hutzler, A. Ravi, A. Collopy, J. Ye, W. Ketterle, and J. M. Doyle, Phys. Rev. Lett. **119**, 103201 (2017).
[27] M. R. Tarbutt, B. E. Sauer, J. J. Hudson, and E. A. Hinds, New J. Phys. **15**, 053034 (2013).
[28] L. Xu, Y. Yin, B. Wei, Y. Xia, and J. Yin, Phys. Rev. A **93**, 013408 (2016).
[29] G. Z. Iwata, R. L. McNally, and T. Zelevinsky, Phys. Rev. A **96**, 022509 (2017).
[30] I. Kozyryev, L. Baum, K. Matsuda, B. L. Augenbraun, L. Anderegg, A. P. Sedlack, and J. M. Doyle, Phys. Rev. Lett. **118**, 173201 (2017).
[31] W. Bu, M. Liu, D. Xie, and B. Yan, Rev. Sci. Instrum. **87**, 096102 (2016).
[32] W. Bu, T. Chen, G. Lv, and B. Yan, Phys. Rev. A **95**, 032701 (2017).
[33] A. Cournol, P. Pillet, H. Lignier, and D. Comparat, arXiv:1709.06797.
[34] L.-E. Berg, N. Gador, D. Husain, H. Ludwigs, and P. Royen, Chem. Phys. Lett. **287**, 89 (1998).
[35] T. Chen, W. Bu, and B. Yan, Phys. Rev. A **94**, 063415 (2016).
[36] D. J. Berkeland and M. G. Boshier, Phys. Rev. A **65**, 033413 (2002).
[37] S. Truppe, H. J. Williams, N. J. Fitch, M. Hambach, T. E. Wall, E. A. Hinds, B. E. Sauer, and M. R. Tarbutt, New J. Phys. **19**, 022001 (2017).
[38] V. Zhelyazkova, A. Cournol, T. E. Wall, A. Matsushima, J. J. Hudson, E. A. Hinds, M. R. Tarbutt, and B. E. Sauer, Phys. Rev. A **89**, 053416 (2014).
[39] D. Xie, W. Bu, and B. Yan, Chin. Phys. B **25**, 053701 (2016).
[40] H. J. Metcalf and P. Straten, *Laser Cooling and Trapping* (Springer, Berlin, 1999).
[41] M. R. Tarbutt, New J. Phys. **17**, 015007 (2015).